Does the transport of dissolved organic nutrients affect export production in the Atlantic Ocean?

Vassil Roussenov,[1] Richard G. Williams,[1] Claire Mahaffey,[2] and George A. Wolff[1]

Received 15 March 2005; revised 9 February 2006; accepted 27 March 2006; published 8 July 2006.

[1] A simplified cycling and transport model for inorganic nutrients and dissolved organic nitrogen (DON) and phosphorus (DOP) is applied to the Atlantic, on the basis of recent measurements along a meridional transect. The DON and DOP are separated into semilabile pools with a lifetime of 6 months and a refractory pool which is conserved in the interior, but photochemically breaks down in the euphotic zone with a lifetime of 6–12 years. The semilabile pool typically only makes up 10% of the surface DON, but up to 95% of DOP. DON and DOP are preferentially produced over upwelling zones in the euphotic zone. Elevated surface concentrations of DON and DOP generally occur over the tropics where the mixed layer is thin, but become diluted at higher latitudes where the mixed layer is thick. There is a northward transport of DON and DOP from the tropics into the northern subtropical gyre, as part of the Ekman wind-driven circulation and overturning circulation. At the same time, there is a depth-integrated southward transport of nitrate and phosphate leading to a loss of nitrate and phosphate over the subtropics of the North Atlantic, which is partly compensated by the supply of DON and DOP. Inputs of DON enhance the particle export over the subtropical gyres by typically 0.05 mol N m^{-2} yr^{-1}, compared with a background model particle export of typically 0.2 mol N m^{-2} yr^{-1}. Inputs of DOP appear to be more significant (owing to their smaller refractory content) in increasing particle export by typically 12 mmol P m^{-2} yr^{-1} over the subtropical gyre, which is sufficiently large to supply half of the phosphorus requirements for particle export.

Citation: Roussenov, V., R. G. Williams, C. Mahaffey, and G. A. Wolff (2006), Does the transport of dissolved organic nutrients affect export production in the Atlantic Ocean?, *Global Biogeochem. Cycles*, *20*, GB3002, doi:10.1029/2005GB002510.

1. Introduction

[2] Dissolved organic nitrogen (DON) and phosphorus (DOP) constitute the largest portion of the nitrogen (N) and phosphorus (P) pools in the surface of oligotrophic subtropical gyres and are therefore potentially important in providing the N and P to phytoplankton in these nutrient impoverished regions. The DON and DOP may be supplied over these large-scale downwelling regions through a lateral transfer from neighboring upwelling zones in the tropics and subpolar gyres [*Williams and Follows*, 1998; *Abell et al.*, 2000]. In addition, DON and DOP may become important in closing N and P budgets over basins, as first proposed for the subtropics of the North Atlantic by *Rintoul and Wunsch* [1991]. While nitrogen fixation might also provide an alternative mechanism to supply the necessary N, there is no equivalent process to supply P.

[3] Identifying the role of DON and DOP, both locally and on the basin scale, has proved difficult through the paucity of direct observations, as well as the uncertainty regarding the reactivity and composition of dissolved organic matter. In this study, we exploit our recent analysis of organic nutrients along a meridional transect through the Atlantic [*Mahaffey et al.*, 2004]. An isopycnic circulation model is coupled with a simplified nutrient model including inorganic nutrients, and semilabile and refractory components of dissolved organic nutrients. As the focus of the model study is on the cycling and transport of dissolved organic nutrients, we do not address the role of potentially other important nutrient sources to the euphotic zone, such as atmospheric deposition, nitrogen fixation and fine-scale upwelling by mesoscale eddies and fronts. This study addresses the following questions: (1) How are surface DON and DOP distributions controlled over the North Atlantic? (2) How does the inclusion of DON and DOP affect the budgets of N and P? (3) How does the incorporation of DON and DOP affect particle export?

[4] In section 2, we review the key observations for DON and DOP in the Atlantic. In section 3, we develop our simplified coupled transport and nutrient cycling model and describe the resulting nutrient distributions. In sections 4 and 5, the role of DON in possibly sustaining particle

[1]Department of Earth and Ocean Sciences, University of Liverpool, Liverpool, UK.
[2]Department of Oceanography, University of Hawaii, Honolulu, Hawaii, USA.

0886-6236/06/2005GB002510$12.00

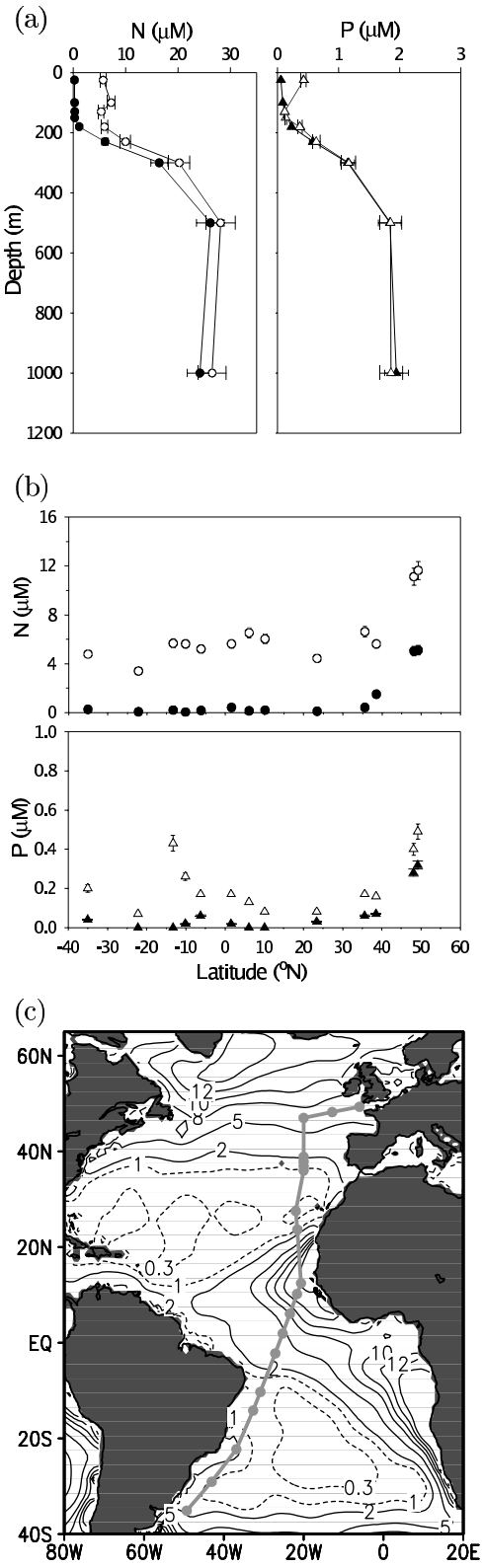

Figure 1. Distributions of nutrients (μM) along the AMT10 transect in spring 2000. (a) (left) Total dissolved nitrogen (TDN) (open circle: μM) and nitrate (solid circle) and (right) total dissolved phosphorus (TDP) (open triangle) and phosphate (solid triangle) in the South Atlantic at 13.51°S, 32.33°W over 1000 m. Error bars are ±1 standard error. (b) (top) Meridional sections of TDN (open circles) and nitrate (NO_3^-; solid circles) and (bottom) TDP (open triangle) and phosphate (PO_4^{3-}; solid triangle) (μM) averaged over the mixed layer through the Atlantic (45°S to 45°N) along the transect. (c) AMT10 cruise track with stations marked superimposed on climatological surface nitrate. Further details are given by *Mahaffey et al.* [2004].

export and closing nutrient budgets is investigated, and in section 6, the role of DOP is similarly assessed.

2. Observations of DON and DOP

2.1. DON and DOP Composition

[5] While DON and DOP are ultimately linked to each other through the formation and cycling of organic matter, they differ in their composition and reactivity. DON consists of a variety of molecules from simple amino acids, neutral and amino sugars to complex humic and uncharacterized protein molecules (see review by *Benner* [2002]). In contrast, DOP consists of nucleic acids, ATP, ADP, cyclic AMP, lipids, vitamins and phosphate polymers (see review by *Karl and Bjorkman* [2002]). The biogeochemistry of the DON and DOP pools result in DON being intrinsically less reactive than DOP. Consequently, there can be a local decoupling of the biological production, recycling and remineralization of N and P.

[6] DON is produced through passive or active exudation by phytoplankton, N_2-fixing organisms, by bacterially mediated processes, photochemical reactions and grazing [*Bronk*, 2002]. N_2-fixing organisms are a significant source of DON, but are P limited, thus leading to elevated surface DON, and possibly drawdown of DOP.

[7] The DON pool is usually separated into labile, semilabile and refractory dissolved organic matter pools. The labile and semilabile pools are reported to be biologically reactive on timescales of hours to days [*Bronk et al.*, 1994] and months to years [*Carlson*, 2002], respectively. Within the ocean interior, there is a large refractory DON pool which has escaped degradation [*Loh et al.*, 2004]. In contrast, nearly all of the DOP pool is considered to be labile or semilabile, with turnover times for the semilabile pool of typically 40 to 300 days [*Bjorkman et al.*, 2000].

2.2. Total Dissolved Nitrogen and Phosphorus Distributions Through the Atlantic

[8] The Atlantic Meridional Transect (AMT10) was surveyed from 35°S, 49°W to 48°N, 20°W in April and May 2000, passing across the subtropical gyre in the South Atlantic and along the eastern flank of the subtropical gyre in the North Atlantic (Figure 1). Total dissolved nitrogen (TDN) and total dissolved phosphorus (TDP) were analyzed from 7 to 10 depths at 23 stations [*Mahaffey et al.*, 2004]. The dissolved organic nitrogen (DON) and phosphorus

Table 1. Concentrations of Dissolved Organic Nitrogen (DON, μM) and Dissolved Organic Phosphorus (DOP, μM) in the Mixed Layer (Upper 100 m) in the Atlantic

Atlantic Region	[DON], μM	Reference
Arctic	3.6 ± 0.4	*Dittmar et al.* [2001]
Arctic	3.6–5.3	*Wheeler et al.* [1997]
Greenland Sea	4.3 ± 0.9	*Lara et al.* [1993]
35°N to 50°N, ~20°W	4.4–7.4	*Kahler and Koeve* [2001]
Sargasso Sea (BATS)	4.0–5.5	*Hansell and Carlson* [2001]
35°S, 49°W to 48°N, 20°W (AMT10)	3.5–6.5	*Mahaffey et al.* [2004]
33°S to 49°N (AMT 11)	3.9–6.8	*Varela et al.* [2005]
Equatorial Atlantic (15°S–15°N)	9.5 ± 4.1	*Vidal et al.* [1999]
Atlantic Region	**[DOP], μM**	**Reference**
Gulf Stream (41°N, 64°W)	0.07–0.10	*Ridal and Moore* [1990]
Sargasso Sea	0.07 ± 0.04	*Wu et al.* [2000]
Sargasso Sea	0.1–0.5	*Cavender-Bares et al.* [2001]
35°S, 49°W to 48°N, 20°W (AMT10)	0.07–0.43	*Mahaffey et al.* [2004]
Equatorial Atlantic (15°S–15°N)	~0.1–0.3	*Vidal et al.* [1999]

(DOP) pools were identified from the difference between total dissolved and dissolved inorganic nutrient concentrations after ultraviolet oxidation [*Sanders and Jickells*, 2000], although this method only recovers typically 60 to 70% for DON.

[9] DON and DOP form the majority of the TDN and TDP pools in near-surface waters (>60% in the upper 80 m) over the subtropical gyres (Figures 1a and 1b). DON concentrations ([DON]) were relatively high in the surface waters (5.58 ± 0.96 μM for depths <180 m) and decreased with depth to a residual pool (2.15 ± 0.3 μM for depth >500 m). Similarly, DOP concentrations ([DOP]) were relatively high in surface waters (0.43 ± 0.15 μM), but very small at depth (<0.02 ± 0.001 μM).

[10] Over the mixed layer, there were relatively high concentrations of TDN and TDP over the southern and northern flanks of the subtropical gyres and local minima toward the centers of the gyres (Figure 1b). Within the mixed layer, DON (55 to 100%) and DOP (67 to 100%) dominated the TDN and TDP pools, respectively, over most of the AMT 10 transect, although NO_3^- and PO_4^{3-} became significant north of 40°N. This [DON] range (3.5 μM to 6.5 μM) is broadly comparable with similar observations over much of the North Atlantic and lower concentrations in the Arctic (Table 1), apart from in the tropics where *Vidal et al.* [1999] detected higher concentrations of 9.5 ± 4.1 μM in the upper 100 m. The [DOP] similarly range from 0.07 to 0.43 μM during AMT 10, which is in broad agreement with other studies in the Atlantic (Table 1). Part of the range and discrepancy in [DON] and [DOP] probably reflects methodological differences in the recovery of these complex organic pools [*Bronk and Ward.*, 2000; *Sharp et al.*, 2002].

[11] The lability of the DON was crudely assessed by determining amino acids concentrations along AMT10, which suggested that dissolved free amino acids [DFAA] contribute <0.6% of the total DON pool, while the total hydrolysable amino acids [THAA] account for <9.9% of the total DON pool [*Mahaffey et al.*, 2004]. Assuming that DFAA and THAA provide lower bounds for the size of the labile and semilabile pools (since other labile fractions of DON such as amino sugars were not determined), then these pools of DON are relatively small, making up typically 1% and 10%, respectively. Given the DON and DOP distributions from this single section, we now employ a model to explore the role of DON and DOP in affecting particle export and the closure of nutrient budgets over the North Atlantic.

3. Model for Inorganic and Dissolved Organic Nutrients

3.1. Model for the Cycling of DON

[12] The total nutrient is separated into a dissolved inorganic nutrient, dissolved organic matter consisting of semilabile and refractory components, and particulate organic matter (POM). Organic matter is only assumed to be formed over the euphotic zone, with a constant thickness of h_e = 100 m. POM is assumed to fall out and be remineralized beneath the euphotic zone, while the dissolved inorganic, semilabile and refractory organic nutrients are transported by the circulation. Henceforth, the nutrient model is assumed to be for N unless otherwise stated.

3.1.1. Within the Euphotic Zone

[13] The conservation equations for each nutrient consist of the temporal change in the tracer, the advection of the tracer (written in divergence form), as well as sources and sinks, which for nitrate appears as

$$\frac{\partial}{\partial t}NO_3^- + \nabla.\left(\mathbf{u}NO_3^-\right) = -G + \beta_s DON_s + \beta_r DON_r, \qquad (1)$$

where **u** is the three-dimensional velocity field. The rate of formation of organic matter, G, is assumed to follow a Michaelis-Menten kinetics,

$$G = \alpha\left(\frac{I}{I+I_o}\right)\left(\frac{NO_3^-}{NO_3^- + NO_{3_o}^-}\right), \qquad (2)$$

where α is the consumption rate, I is the intensity of radiation and NO_3^- is the nitrate concentration within the euphotic zone. This form represents how the growth rate depends separately on the irradiance and nitrate concentration, and how the growth rate saturates for high irradiance or high nitrate concentration; fixed value of $\alpha = 1.2 \times 10^{-6}$ μM s^{-1}, I_o = 10 Wm^{-2}, $NO_{3_o}^-$ = 1.5 μM are chosen in order to obtain a maximum in the annually averaged export production of 0.4 mol N m^{-2} yr^{-1}.

[14] The formation of organic matter is separated into fractions, a_{PON} and a_{DON}, passing into PON and DON respectively (where $a_{PON} + a_{DON} = 1$). The DON is further separated into fractions, c_s and c_r, passing into the semilabile and refractory pools, where $c_s + c_r = 1$ and the subscripts s and r refer to the semilabile and refractory components.

$$\begin{aligned} \frac{\partial}{\partial t} DON_s + \nabla.(\mathbf{u} DON_s) &= a_{DON} c_s G - \beta_s DON_s \\ \frac{\partial}{\partial t} DON_r + \nabla.(\mathbf{u} DON_r) &= a_{DON} c_r G - \beta_r DON_r. \end{aligned} \tag{3}$$

In turn, the DON is assumed to breakdown and be consumed at a rate, β, which appears as a source of nitrate in (1), with the lifetimes of the semilabile and refractory DON assumed to be $\beta_s^{-1} = 6$ months and $\beta_r^{-1} = 6$ to 12 years, varying according to the irradiance. This simple closure avoids a proper representation of the microbial loop and conversion of DON to ammonium.

3.1.2. At the Base of the Euphotic Zone

[15] Our focus is on the PON formed over the euphotic zone and exported through fallout, referred to as the particle export, $F(-h_e)$, given by

$$F(-h_e) = a_{PON} \int_{z=-h_e}^{z=0} G(z) dz, \tag{4}$$

and, likewise, on the DON formed over the euphotic zone given by

$$a_{DON} \int_{z=-h_e}^{z=0} G(z) dz. \tag{5}$$

The export production is defined as the physical flux of organic matter through the base of the euphotic zone given by the sum of the particle flux, the downward transport and diffusive transfer of DON,

$$F(-h_e) - wDON + \kappa \frac{\partial}{\partial z} DON, \tag{6}$$

where κ is the vertical diffusivity (a more complicated representation of the diffusive transfer occurs if there is convection). However, in practice, this flux given by (6) is difficult to measure and, instead, we focus on the production and export of PON (4) and the production of DON (5).

3.1.3. Below the Euphotic Zone

[16] Below the euphotic zone, the PON fallout flux is assumed to exponentially decay with depth down to the top of the densest model interface,

$$F(z) = F(-h_e) \exp(\gamma(z + h_e)), \tag{7}$$

with a remineralization depth scale given by γ^{-1} and the flux assumed to vanish at the seafloor, so that there is no loss term of nutrients within the water column. The remineralization of PON is then given by the vertical convergence of the PON flux, $\frac{\partial F}{\partial z}$. The remineralization scale, γ^{-1}, is chosen to be 200 m, which is close to the vertical scale of 165 m diagnosed in the Subduction Region of the northeast Atlantic [*Jenkins*, 1998]. Our choice of γ^{-1} suggests that less than 1% of PON export from the euphotic zone passes below 1000 m in the model.

[17] The remineralization process involves the microbially mediated transfer of organic bound N to inorganic N. The pathways of remineralization are complex and involve two processes: ammonification, the breakdown of organic N to ammonium, and nitrification, a two-step process involving ammonium oxidation and nitrite oxidation. As our focus is on new and export production, we have omitted ammonium and nitrite as intermediary products of remineralization, which are associated with regenerated production. Thus the remineralization of PON is assumed to provide a source of nitrate. In addition, the semilabile DON is also converted to nitrate with a decay rate β_s, while the refractory DON is assumed to be conserved,

$$\begin{aligned} \frac{\partial}{\partial t} NO_3^- + \nabla.\left(\mathbf{u} NO_3^-\right) &= \frac{\partial F}{\partial z} + \beta_s DON_s, \\ \frac{\partial}{\partial t} DON_s + \nabla.(\mathbf{u} DON_s) &= -\beta_s DON_s, \\ \frac{\partial}{\partial t} DON_r + \nabla.(\mathbf{u} DON_r) &= 0. \end{aligned} \tag{8}$$

The N cycling model includes a crude representation of a diurnal cycle where each day is separated into a light and dark period. Organic matter is produced and released in the euphotic zone only when there is light. The resulting PON falls out and is remineralized into nitrate, then is physically transferred by the convection and circulation. The remineralized nitrate is only returned back to the euphotic zone during the nighttime in order to represent the diurnal cycle in convection.

3.2. Biochemical Justification for Model Parameters

[18] The nutrient model parameters used for the cycling of nitrate are simple choices to close the system and are not new. However, the parameter choices for the DON partitioning in (3) are more novel and require further justification.

3.2.1. What Is the Relative Fraction of Nitrate Passing Into DON and PON?

[19] There is little consensus on how much utilized nitrate is converted into DON [*Bronk*, 2002]. Incubation experiments suggest that between 10 and 40% of DON is released independent of the environment [*Bronk and Ward*, 2000]. However, nutrient and light stress cause cell lysis and DON release, which might occur particularly in oligotrophic water, suggesting that these incubation experiments might provide a lower bound for DON release. Estimates of DON release increase from low values of 8 to 19% in eutrophic waters in the Ross Sea [*Hu and Smith*, 1998] to higher values ranging from 26% to 100% in oligotrophic waters [*Raimbault et al.*, 1999].

[20] Over the Atlantic, one expects that the relative fraction of nitrate forming DON will change with the

background availability of nitrate. The standing stocks of DON and PON vary strongly with the environment: In eutrophic waters, the concentrations of PON and DON are comparable, typically 5 μM and 5 to 10 μM, respectively, while in oligotrophic environments, the concentration of PON is much reduced, typically 0.1–0.2 μM, while DON is typically 6–8 μM. Thus the ratio of PON and DON changes from 1:1 or 1:2 in a eutrophic environment to 1:30 or 1:80 in an oligotrophic environment. However, these ratios reflect the concentration of the standing stocks, rather than the fluxes and rates of turnover.

[21] The change in PON and DON cycling is more likely to be reflected by the e-ratio, defined as the ratio of particle export and primary production, which decreases from a high value in eutrophic waters to a low value of 0.1 to 0.2 in oligotrophic waters. Consequently, in our model, we assume that the fraction of PON formed from the total organic matter produced is 50% in eutrophic water and decreasing to 35% in oligotrophic waters, with the remaining organic matter formed as DON; in (3), this separation is represented as $a_{PON} = 0.5$ for surface $[NO_3^-] > 5$ μM and $a_{PON} = 0.35$ with $[NO_3^-] < 5$ μM.

3.2.2. What Are the Proportions of Labile, Semilabile, and Refractory DON Exuded?

[22] Culture studies suggest that phytoplankton exude 7 to 15% and 18 to 37% of DON in the form of free amino acids and combined amino acids, respectively, suggesting that 25 to 52% of DON released is labile [*Flynn and Berry*, 1999]. It is unclear as to the partitioning of the remainder of the exuded DON between the semilabile and refractory forms. In addition, there are biochemical transformations of the exuded labile and semilabile DON to refractory DON within the water column [*Benner*, 2002].

[23] In our model, we choose that 50% of DON formed is semilabile and the remainder is refractory; thus, $c_s = 0.5$ in (3). This partitioning is poorly known and has been tuned to provide reasonable background concentrations in refractory DON within the model. The labile fraction is omitted in the model, since it is rapidly utilized on a timescale of only a few hours that is too short a time for any significant transport to occur.

3.2.3. What Is the Rate of Photochemical Breakdown of Refractory DON?

[24] Refractory DON is assumed to be conserved in the ocean interior and subject to photochemical break down in the photic zone. Photodegradation of DOC is measured to occur at a rate of typically 20 nM per hour [*Mopper et al.*, 1991]. Assuming that the rate of photooxidation of DON and DOC are both limited by ultraviolet absorption, then following *Mopper et al.* [1991], assuming an irradiance of 170 W m^{-2} of solar noon radiation at 26°N, the accompanying UV-B radiation implies that the 5 μM of refractory DON would have a lifetime of only10 days. However, if the DON is mixed over a depth of $h \sim 100$ m, then the lifetime increases by the factor $h\gamma \sim 30$ to typically 1 year. In addition, there are only 2 to 4 hours of peak irradiance per day, implying that the lifetime of refractory DON is 6 to 12 years; thus β_r^{-1} in (3) is chosen to vary over this range according to the local irradiance.

3.3. General Circulation Model

3.3.1. Model Formulation

[25] The model study employs an isopycnic model (MICOM 2.7 [*Bleck and Smith*, 1990]). The model includes 15 isopycnal layers in the vertical plus a surface mixed layer with variable density. The potential density layers are referenced to a depth of 2 km. The model resolution is 1.4° in the horizontal on a Mercator grid (150 km at the equator and 75 km at 60°N) with a topography based on ETOP05 data. There is a diapycnic diffusivity, $\kappa = 10^{-7}/N$, varying with buoyancy frequency N, which typically varies from 10^{-5} m^2 s^{-1} in the thermocline to 10^{-4} m^2 s^{-1} in the deep waters, as well as isopycnic mixing and thickness diffusion; see *Williams et al.* [2006] for further details of the physical model.

[26] The model is forced using monthly wind stress, surface freshwater fluxes, surface radiative fluxes, with latent and sensible heat fluxes calculated from air temperature and water vapor mixing ratio from NCEP. On the northern and southern boundaries, there is a ''sponge relaxation'' to climatology (relaxation timescale increasing from 30 to 180 days) for temperature in the mixed layer, salinity and the height of density interfaces for all layers. Rivers are added as freshwater fluxes at corresponding grid points. The Strait of Gibraltar is closed, but the salinity of subsurface layers close to there is relaxed to climatology on a 30-day timescale. The model is initialized from Levitus climatology (temperature, salinity and density) and integrated for an initial spinup of 60 years and then a further 40 years using the coupled circulation and nutrient model.

3.3.2. Model Circulation

[27] The depth-integrated transport reveals the classical wind-driven, anticyclonic circulation over the subtropical gyre (10°N to 40°N–50°N) and cyclonic circulation over the subpolar gyre (Figure 2a). The depth-integrated horizontal transport reaches 40 Sv (1 Sv = 10^6 m^3 s^{-1}) over the Gulf Stream, which is consistent with the wind stress curl forcing. There is not the observed enhancement of the boundary current transport here to perhaps 100 Sv owing to the relatively coarse horizontal resolution. The transport over the mixed layer reaches a maximum of 8 Sv with transport contours aligned meridionally over the eastern side of the subtropical gyre reflecting the wind-driven Ekman contribution (Figure 2b).

[28] As well as the horizontal circulation, there is an overturning driven by the buoyancy forcing reaching a maximum value of 13 Sv (Figure 2c). The overturning leads to a northward flux of light fluid and a southward flux of denser fluid.

3.4. Model Experiments for DON and DOP

[29] The coupled circulation and nutrient model carries tracers for nitrate, refractory DON and semilabile DON, which are integrated on line for a further 40 years. The initial nitrate is taken from Levitus climatology (NODC), while the semilabile and refractory DON is initialized, respectively, to 0 and 1 μM everywhere. Subsequent plots are usually for an annual mean average over the last 5 years of model integration.

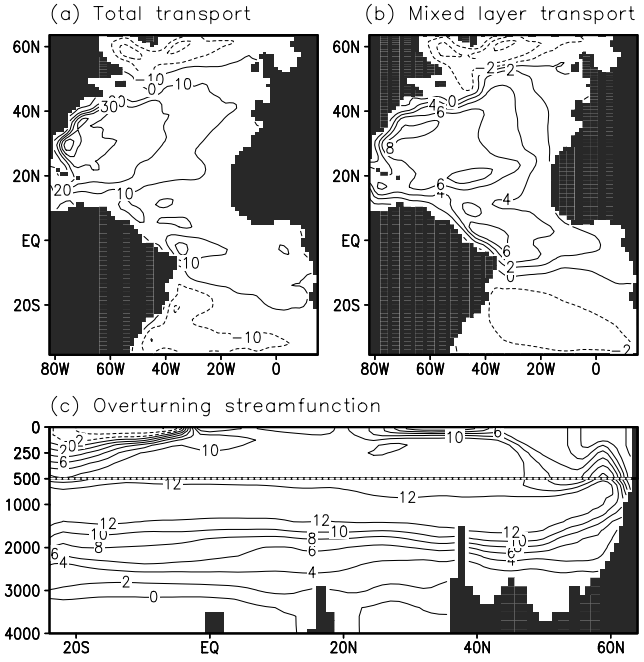

Figure 2. Model circulation after 100 years integration (1 Sv = 10^6 m^3 s^{-1}). (a) Horizontal transport integrated over the water column. (b) Horizontal transport integrated over the mixed layer. (c) Overturning transport for depth versus latitude (with an expanded scale in the upper 500 m).

[30] The model integration broadly captures the observed meridional structure of the nitrate distribution (Figure 3a). There is a plume of high nitrate associated with a combination of Sub-Antarctic Mode Water (SAMW) and Antarctic Intermediate Water (AAIW) passing into the domain from 20°S at depths from 500 m to 1500 m. In the climatological data and the model, the plume becomes diluted north of the equator at 20°N and 10°N, respectively. In deep waters below 500 m, the lowest nitrate concentrations are in the subpolar gyre, reflecting the relatively recent ventilation and low age there.

[31] The model reveals the expected low concentrations of surface nitrate over the subtropical gyres and higher concentrations at high latitudes and over the upwelling zones along the eastern boundary (Figure 3b). In both the data and the model, there is the expected northward increase in nitrate concentrations associated with the thickening of the winter mixed layer over the North Atlantic. There is good agreement between the model for the tropics over the upper 100 m and the climatological data (Figure 3c), apart from over the northern subtropical gyre where the model overestimates the surface nitrate concentrations.

[32] The model shows that there are generally high concentrations of the annually averaged DON in the tropics and lower concentrations at higher latitudes (Figure 4a). In the tropics and eastern side of the subtropical gyres, there is lower [DON] in the surface waters locally over the strong upwelling zones off Africa, reflecting the input of deep waters with low [DON]. Owing to the high concentrations of nitrate in these upwelling zones, there is enhanced formation of DON here (see Figure 6b in section 5.1) and the newly formed DON is laterally transported within the mixed layer. DON concentrations become highest in the surface waters in the tropics away from the local upwelling zones, but become low at higher latitudes owing to the thick mixed layers and the dilution from convection. The high [DON] from the tropics is then transported northward into the subtropical gyre.

[33] The fraction of semilabile DON ranges between 6% and 16% with low fractions over the downwelling regions of the subtropical gyres, but reaches higher fractions over the tropical and coastal upwelling zones (Figure 4b). The higher fractions of semilabile DON over the upwelling zones reflects the recent formation of DON there. This model range for semilabile [DON] is broadly in accord with amino-acid analyses from AMT10 providing a lower bound of 10% semilabile DON [*Mahaffey et al.*, 2004].

[34] Along the AMT10 section, there are broadly similar background patterns in [DON] in the data and model over

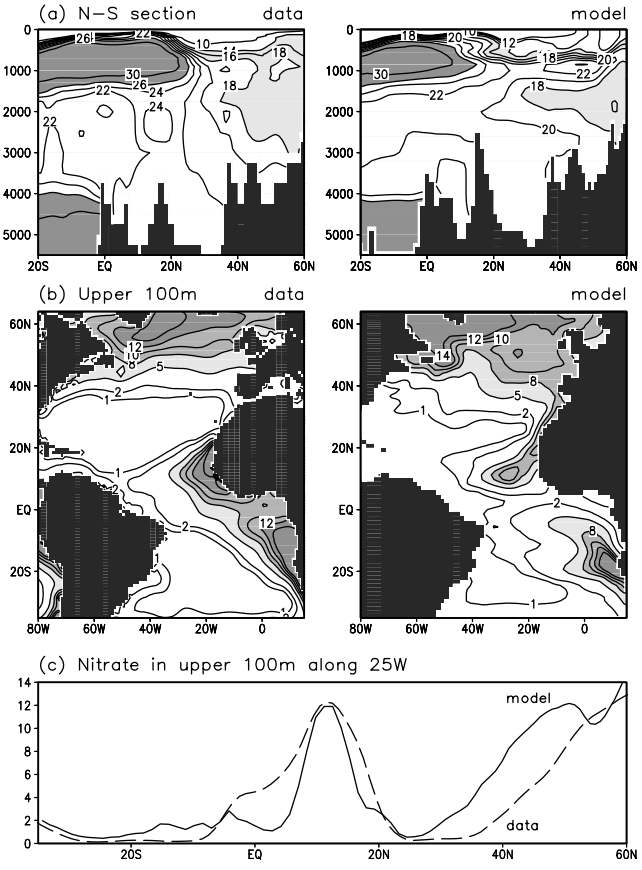

Figure 3. (left) Nitrate distributions (μM) from climatology and (right) the default model integration for (a) meridional section along 25°W and (b) maps of nitrate concentration in the upper 100 m, together with (c) nitrate concentration in the upper 100 m along 25°W for climatology (dashed line) and the model (solid line). The model integration has 60 years dynamical spinup and a further 40 years of coupled circulation and nutrient integration.

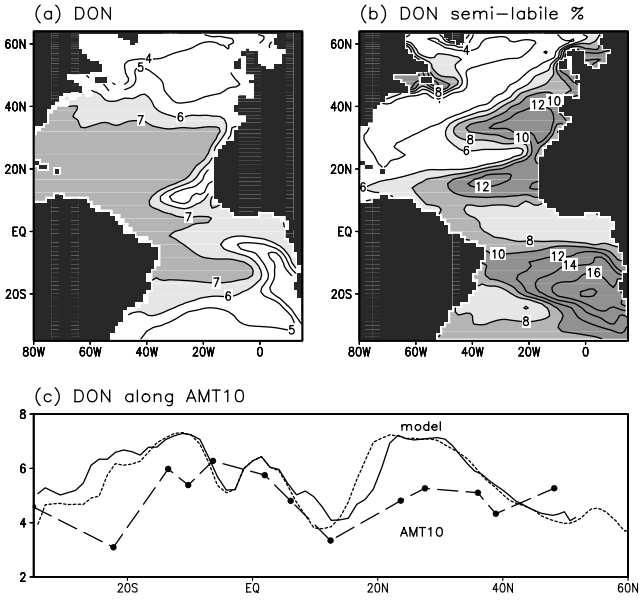

Figure 4. Model distributions for (a) DON (μM) and (b) percentage of semilabile DON, together with (c) DON concentrations over the upper 150 m along the AMT10 track from the data (dashed line with stations marked) and the model (solid line along the AMT track and dotted line along 25°W).

the upper 150 m (Figure 4c), although the model has higher [DON] over the subtropical gyres. While acknowledging that there are some limitations in the model simulation for nitrate and DON, the model is now used to explore how the cycling and transport of DON affects the N budget and PON export over the subtropical North Atlantic.

4. Role of DON in Closing the N Budget

4.1. Meridional Fluxes of Nitrate

[35] Nitrate concentrations are elevated in the subpolar gyre and deep waters, but depleted over the surface waters and subtropical gyres (Figure 5a). Over the upper 100 m, the zonally integrated flux of nitrate is rather weak and usually less than 50 kmol N s^{-1} (Figure 5c, solid line).

[36] Over the Atlantic, the model provides a southward transport of nitrate, consistent with the overturning circulation and vertical contrasts in nitrate. The depth and zonally integrated nitrate flux reaches −40 kmol N s^{-1} at 20°S, increasing in magnitude to −140 kmol N s^{-1} at 18°N, then −107 kmol N s^{-1} at 24°N and decreasing to zero at 65°N (Figure 5d, short-dashed line). This overall southward transport of nitrate is achieved by a southward, zonally integrated flux of nitrate below 1500 m, reaching −240 kmol N s^{-1} at 20°S and −200 kmol N s^{-1} at 24°N, associated with the southward transport of North Atlantic Deep Water. This southward transport of nutrient-rich deep waters exceeds the northward zonally integrated flux of nitrate occurring over the upper 1500 m, reaching 200 kmol N s^{-1} at 20°S and 93 kmol N s^{-1} at 24°N, associated with the northward transport of SAMW and AAIW.

[37] Our model solutions are broadly in accord with recent observational analyses suggesting a southward nitrate flux of −130 kmol N s^{-1} across 24°N [*Lavín et al.*, 2003] and −50 kmol N s^{-1} across a section from Spain to Greenland of [*Álvarez et al.*, 2002]. In contrast, *Rintoul and Wunsch* [1991] diagnosed a northward nitrate flux of 120 kmol N s^{-1} at 36°N and a weak southward flux of −8 kmol N s^{-1} at 24°N on the basis of a combination of an inverse model and hydrographic data. These different directions of the net nitrate flux reflect how the overturning circulation and horizontal circulations partly oppose each other: The overturning provides an overall southward nitrate flux and the horizontal, "gyre" circulation a northward nitrate flux. In our model, the overall southward transport

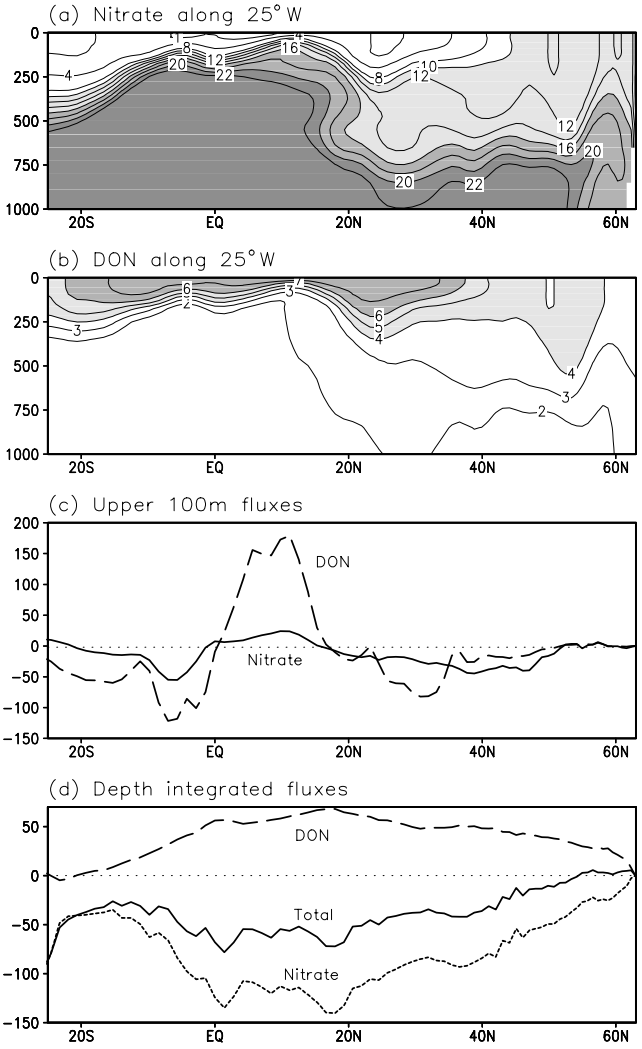

Figure 5. Modeled (a) nitrate and (b) DON sections over the upper 1000 m along 25°W in the North Atlantic, (c) zonally integrated northward flux of nitrate (solid line) and DON (dashed line) (10^3mol N s^{-1}) over the upper 100 m, and (d) zonally and depth-integrated northward flux for nitrate (10^3mol N s^{-1}, short-dashed line), DON (long-dashed line), and TDN (solid line) over the whole water column.

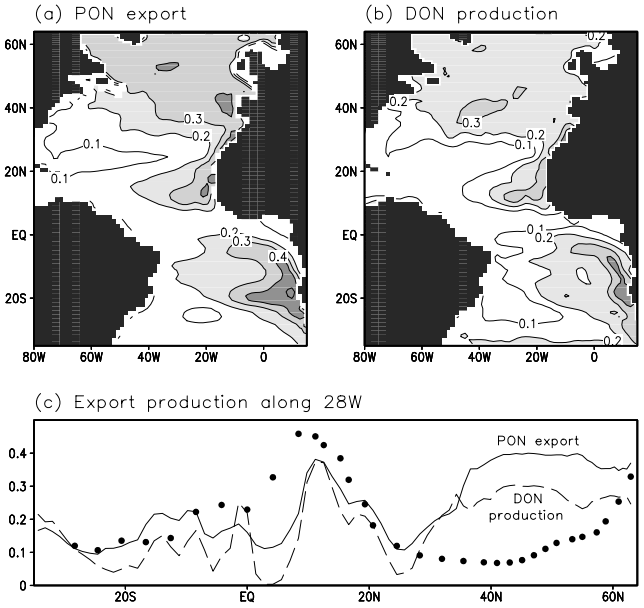

Figure 6. Modeled maps for (a) annual export of particulate organic matter (PON) at a depth of 100 m (mol N m^{-2} yr^{-1}), (b) production of DON (mol N m^{-2} yr^{-1}), and (c) modeled PON export (solid line) and DON production (dashed line) along 28°W, compared with inferred PON export from the inverse study of *Schlitzer* [2000] (dotted line).

of nitrate is a direct consequence of the overturning circulation (Figure 2b), dominating over the horizontal gyre circulation, but this result might partly be a consequence of the coarse horizontal resolution. Despite differences in the direction of the nitrate transport, all the studies suggest that there is a loss of nitrate over the subtropical North Atlantic, which requires an additional N source for a steady state to be attained.

4.2. Meridional Fluxes of DON

[38] The different nitrate and DON distributions over the upper ocean lead to contrasting fluxes. DON concentrations are highest in the surface waters in the tropics and lowest in deep waters and high latitudes (Figure 5b). Over the upper 100 m, DON is fluxed northward from the tropics to the northern high latitudes reaching 179 kmol N s^{-1} at 12°N (Figure 5c, dashed line). Thus the near-surface advection of DON provides a source of N over the northern subtropical gyre. The depth and zonally integrated DON flux over the whole water column is likewise directed northward over most of the Atlantic, with a maximum value of 68 kmol N s^{-1} at 18°N and reducing to zero at 65°N (Figure 5d, dashed line). Thus, in the model, the transport of DON provides a depth-integrated supply of N to the subtropical North Atlantic. This result is in accord with the hypothesis by *Rintoul and Wunsch* [1991], who suggested that the loss of nitrate in the subtropical North Atlantic might be closed by a compensating supply of DON, although nitrogen fixation could provide a similar role.

[39] In the model, this supply of N associated with the DON transport partly offsets the loss of nitrate, but there is still an overall loss of N associated with the southward flux of TDN reaching −72 kmol N s^{-1} at 18°N (Figure 5d, solid line). The overall loss of N from the model domain is due to the southern boundary condition allowing an outflux of nitrate. For a steady state, there needs to be a compensating external input of N, such as from atmospheric deposition, nitrogen fixation or river inputs. Consequently, while these model calculations illustrate the role of DON, the absolute values should be viewed with some caution, as the model does not include external sources of N and P.

5. Role of DON in Sustaining Export Production

5.1. PON Export and DON Production

[40] The modeled PON export typically ranges from 0.19 mol N m^{-2} yr^{-1} over much of the tropical and subtropical Atlantic and increases to 0.31 mol N m^{-2} yr^{-1} over higher latitudes (Figure 6a and Table 2). The local maxima in PON export are connected with upwelling zones off Africa or with regions of strong convection north of 40°N. The local minima in PON export occurs over the remote western and central parts of the subtropical gyres where there is both large-scale downwelling, limited convection and where any lateral transfer of inorganic nutrients has become exhausted in the surface waters [*Williams and Follows*, 1998].

[41] There is a broadly similar pattern in DON production with elevated rates in the subpolar gyre and upwelling zones off Africa (Figure 6b), which is to be expected given the model closures adopted in (3). This pattern is in contrast to that of [DON] in the upper 100 m (Figure 4a), which also reflects the affect of the mixed layer thickness in concentrating DON in the tropics and diluting it at high latitudes.

[42] The area-integrated PON export reaches 137 kmol N s^{-1} over the subtropical area from 15°N to 45°N, compared with 122 kmol N s^{-1} over the tropics from 15°S to 15°N and 82 kmol N s^{-1} in the subpolar gyre from 45°N to 65°N (Table 2). Thus the area-integrated PON export and DON production over the North Atlantic is dominated by the subtropical gyre contribution owing to its extensive area.

[43] It is difficult to assess the realism of the modeled PON export and DON production. Along the eastern

Table 2. Model Estimates for PON and PP Export and DON and DOP Production for Latitude Bands Over the Atlantic in Terms of an Area Average or Area-Integrated Flux

		PON, PP Export		DON, DOP Production	
Region	Area, 10^6 km^2	Average, mmol m^{-2} yr^{-1}	Integral, kmol s^{-1}	Average, mmol m^{-2} yr^{-1}	Integral, kmol s^{-1}
45°N–65°N	8.3	310, 20.1	82, 5.4	250, 12.9	67, 3.5
15°N–45°N	23.4	180, 18.9	147, 14.2	150, 10.4	100, 7.1
15°S–15°N	19.5	200, 18.0	122, 11.2	140, 9.1	90, 5.7

Atlantic, the modeled PON export varies from 0.38 mol Nm^{-2} yr^{-1} in the tropics, reducing to less than 0.15 mol Nm^{-2} yr^{-1} over the subtropical gyres and increasing to nearly 0.4 mol Nm^{-2} yr^{-1} north of 40°N (Figure 6c, solid line). The DON production varies in a similar manner, but with the minimum in DON production reaching 0.05 mol Nm^{-2} yr^{-1} over the subtropical gyres (Figure 6c, dashed line).

[44] In comparison, independent transient-tracer and oxygen observations over the Sargasso Sea reveal higher values in export production reaching 0.48 ± 0.14 mol N $m^{-2}yr^{-1}$ [*Jenkins*, 1982, 1988; *Jenkins and Goldman*, 1985]. Even if our model estimates of export production are taken as a sum of the PON export and DON production, then they only typically reach between 0.2 and 0.3 mol Nm^{-2} yr^{-1}. Thus the model requires additional N supplies to the euphotic zone, such as nitrogen fixation [*Gruber and Sarmiento*, 1997] and possibly contributions from fine-scale, transient upwelling associated with mesoscale eddies [*McGillicuddy et al.*, 1998], frontal features [*Lévy et al.*, 2001] or enhanced diapycnic diffusion from double diffusion [*Dietze et al.*, 2004]. However, our modeled PON export of between 0.1 and 0.2 mol Nm^{-2} yr^{-1} compares reasonably with floating, surface tethered traps measurements at Bermuda (31.5°N, 64.1°W) of PON export of 0.12 and 0.06 mol N m^{-2} yr^{-1} at depths of 150 m and 400 m, respectively [*Usbeck et al.*, 2003].

[45] Alternatively, our model estimates of PON export appear to be broadly similar to independent model studies over the tropics and high latitudes, but provide larger estimates over the subtropical gyres. For example, inverse model studies by *Schlitzer* [2000] and *Usbeck et al.* [2003] estimate a PON export of less than 0.1 mol N m^{-2} yr^{-1} over much of the subtropical gyres, increasing to 0.35 mol N m^{-2} yr^{-1} at 60°N, and more than 0.4 mol N m^{-2} yr^{-1} over the upwelling zones off Africa (Figure 6c, dotted line). In addition, *Oschlies* [2002] employed a 1/9°, eddy-resolving experiment for the North Atlantic and obtained a total nitrate input into the euphotic zone of less than 0.05 mol N m^{-2} yr^{-1} over the subtropical gyre between 15°N and 30°N, increasing to greater than 0.5 mol N m^{-2} yr^{-1} north of 40°N.

5.2. Sensitivity of PON Export to the Cycling of DON

[46] Our hypothesis is that the inclusion of DON leads to enhanced PON export over the subtropical gyres through the lateral influx of semilabile DON. However, it is difficult to assess the role of DON inputs based on the preceding model integration due to the dominant role of nitrate in sustaining PON export over most of the Atlantic. In order to test this hypothesis, we now consider idealized experiments where the DON is artificially considered either to be entirely refractory or entirely semilabile.

[47] When there is 100% semilabile DON, there is more active cycling of DON (Figure 7, left). Surface nitrate is increased in concentration over the subtropical gyres, at the expense of DON concentrations. In turn, the increased surface nitrate concentrations leads to enhanced PON export over most of the Atlantic (Figure 7c). Conversely, when there is no semilabile DON, DON acts as a chemically inert tracer and does not contribute to export production. Surface nitrate concentrations are reduced over the subtropical gyres, DON concentrations become elevated over the tropics and PON export is reduced (Figure 7c, right).

[48] Incorporating semilabile DON in the model clearly leads to enhanced PON export, as reflected by comparing the default model integration (Figure 6a) and the artificial case with 0% semilabile DON (Figure 7c). The difference in PON export between these two model integrations reveals that incorporating semilabile DON leads to an enhancement in PON export reaching between 0.05 and 0.1 mol N m^{-2} yr^{-1} over the subtropical gyres (Figure 8a). Thus inputs of DON account for typically 40% of the PON export in the default model integration (Figure 8b).

[49] The enhancement in PON export is achieved through the transport and cycling of semilabile DON. In the model, the transported DON is recycled to nitrate, which in turn forms more DON and PON within the euphotic zone, and so the feedback cycle progresses. The zonally and depth-integrated flux of semilabile DON is northward in the tropics, reaching nearly 10 kmol Ns^{-1}, and reduces to zero close to 40°N (Figure 8c). As the fraction of semilabile DON increases, this northward flux likewise increases and thus sustains a larger PON export over the subtropical gyre.

6. Role of DOP in Sustaining Phosphorus Budgets and Export Production

[50] The role of DOP transport is now similarly considered in terms of its possible impact for the export of particulate organic phosphorus (PP).

6.1. Cycling of DOP

[51] Time series studies in the tropical North Pacific reveal that nearly all DOP is biologically available, with turnover times on the scale of 40 to 300 days [*Bjorkman et al.*, 2000]. The refractory organic phosphorus pool, defined as the concentration of DOP in the deep ocean, has been measured as 0.02 μM in the Atlantic [*Mahaffey et al.*, 2004] and 0.04 μM in the Pacific [*Thomson-Bulldis and Karl*, 1998]. From the vertical profile from AMT10, the DOP concentration is 0.43 μM at the surface and 0.02 μM in the deep waters, thus suggesting that the semilabile and refractory pools of organic phosphorus represents 95% and 5%, respectively. However, along AMT10, the minimum surface DOP concentration is 0.07 μM, which suggests that the refractory fraction might possibly locally rise to 28%.

6.2. Phosphate and DOP Distributions

[52] A model integration for phosphate and DOP is now conducted in a similar manner to the previous nitrate and DON integrations. The model integration now assumes that the DOP is 95% semilabile and is initialized with DOP = 0.02 μM and climatological phosphate. After 40 years integration, the surface phosphate has a similar pattern to that of surface nitrate with high concentrations over the upwelling zones off Africa and north of 40°N (Figure 9a). The DOP distribution is again enhanced over the tropics, away from the upwelling zones off Africa, reaching 0.18 μM and decreases to less than 0.12 μM north of 40°N (Figure 9b). In comparison, the observations reveal broadly similar

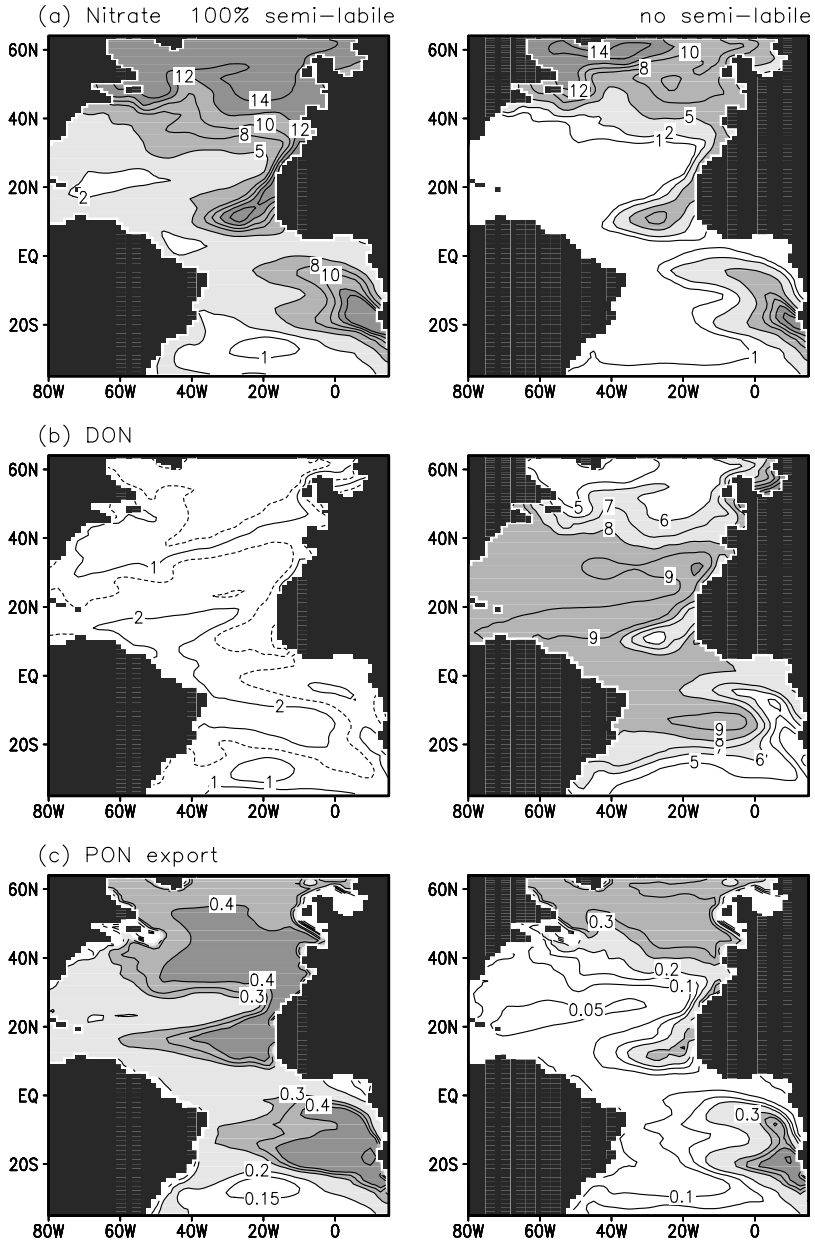

Figure 7. Model sensitivity studies with (left) 100% semilabile DON or (right) no semilabile DON: maps of annual average concentrations (μM) in the upper 100 m for (a) nitrate and (b) DON, together with (c) PON export (mol N m^{-2} yr^{-1}).

values in the tropics of 0.1 to 0.3 μM [*Vidal et al.*, 1999] and a range of 0.07 to 0.43 μM from AMT10 [*Mahaffey et al.*, 2004] (Table 1). The modeled distribution of DOP has a similar range to that of the AMT10 data, but overestimates the [DOP] over the subtropical gyres by 0.1 μM (Figure 9c).

6.3. Transport of DOP

[53] In our model, the flux of DOP over the upper 100 m reaches 4.4 kmol P s^{-1} at 12°N and reducing to zero around 40°N (Figure 9d). This direction of the upper ocean flux of DOP is likewise reflected in a northward depth-integrated flux of DOP reaching 2 kmol P s^{-1} at 12°N decreasing to 0 at 35°N (Figure 9e, dashed line). Consequently, there is a supply of P to the subtropical gyre from the inputs of DOP reaching typically 5.9 mmol P m^{-2} yr^{-1} over the upper 100 m.

[54] In comparison, *Mahaffey et al.* [2004] diagnosed a smaller surface Ekman flux of DOP from AMT10 data providing a DOP supply of 3.4 and 0.92 mmol P m^{-2} yr^{-1} over the southern and northern Atlantic subtropical gyres respectively. In the North Pacific, *Abell et al.* [2000] likewise diagnosed that the supply of TOP reached 4.4 ± 1 mmol P m^{-2} yr^{-1}, which they argued could account for

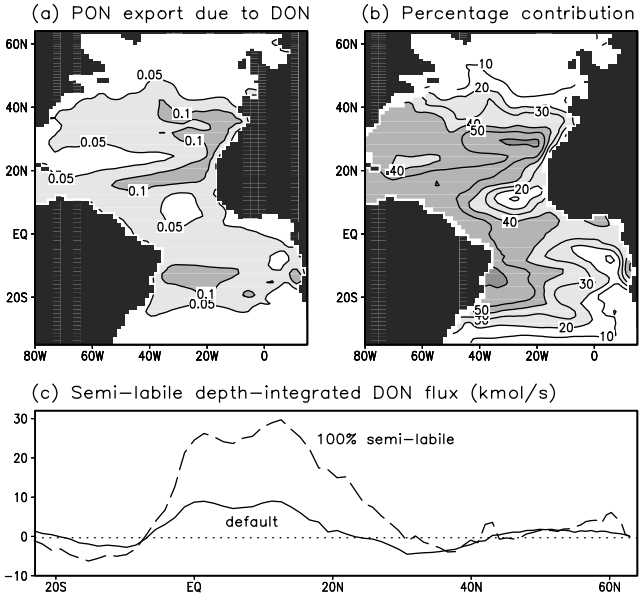

Figure 8. Model estimates of how much PON export (mol N m^{-2} yr^{-1}) is sustained through the supply of semilabile DON: (a) a model estimate based on the difference between modeled PON export from the default model integration and a model integration with no semilabile DON (from Figure 6a minus Figure 7c) and (b) the percentage contribution that DON inputs make to PON export, as well as (c) the depth and zonally integrated flux of semilabile DON (10^3 mol N s^{-1}) for the default model case (solid line) and for 100% semilabile DON (dashed line).

between 40% and 80% of the P needed for particulate export over the subtropical gyre.

6.4. Role of DOP Inputs for PP Export

[55] The modeled PP export reaches 24 and 28 mmol P m^{-2} yr^{-1} around 40°N and the upwelling zones off Africa, and elsewhere reduces to less than 16 mmol P m^{-2} yr^{-1} over parts of the subtropical gyres (Figure 10a and Table 2). If the model integration is repeated without any semilabile DOP being included, then the PP export reduces to <8 mmol P m^{-2} yr^{-1} over much of the subtropical gyres and tropics (Figure 10b).

[56] The PP export due to DOP inputs is revealed by the difference in the PP export in these two integrations, which typically reaches between 8 and 16 mmol P m^{-2} yr^{-1} over the subtropical gyres (Figure 10c). Thus the DOP input accounts for typically 70% of the P supply over the subtropical gyre in our model integration (Figure 10d). Consequently, this model study suggests that the cycling and transport of DOP plays a central role in providing the P needed for export production over subtropical gyres.

7. Discussion

[57] The model study provides a simple representation of the cycling and transport of DON and DOP in order to address their effects on nutrient budgets for the subtropics and particle export over the Atlantic. The DON and DOP distributions reflect a competition between their biological sources and sinks, and their basin-scale transport and convective mixing (Figure 11a). There are high rates of formation of DON and DOP over the upwelling zones in the tropics, subpolar gyre and along the eastern boundary of the subtropical gyres. Over the tropics, there is generally high [DON] and [DOP] within the thin mixed layer away from the local upwelling zones. Farther north in the subpolar gyre, [DON] and [DOP] become low in the surface waters, despite the high levels of biological production, owing to winter convection diluting DON and DOP over the thick mixed layers. The high [DON] and [DOP] from the tropics

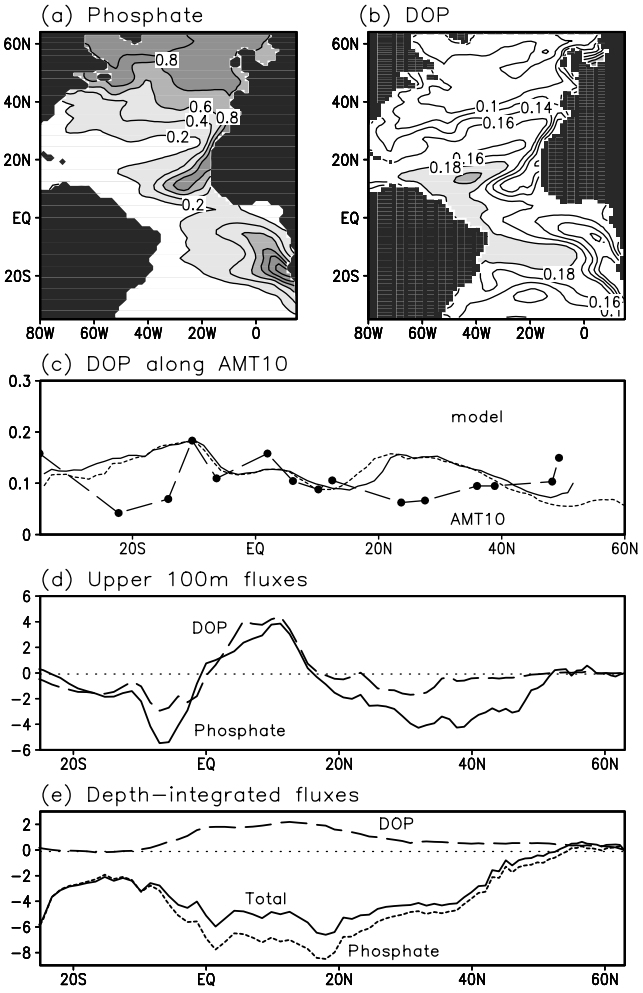

Figure 9. Model distributions for (a) phosphate (μM), (b) DOP (μM), and (c) DOP (μM) concentrations over the upper 150 m for AMT10 data (long-dashed line with stations marked by dots) and from the model (solid line along the AMT track and short-dashed line along 25°W), (d) zonally integrated northward flux of phosphate (solid line) and DOP (dashed line) (10^3mol P s^{-1}) over the upper 100 m, and (e) zonally and depth-integrated northward flux of phosphate (short-dashed line), DOP (long-dashed line), and TDP (solid line) (10^3mol P s^{-1}) over the whole water column.

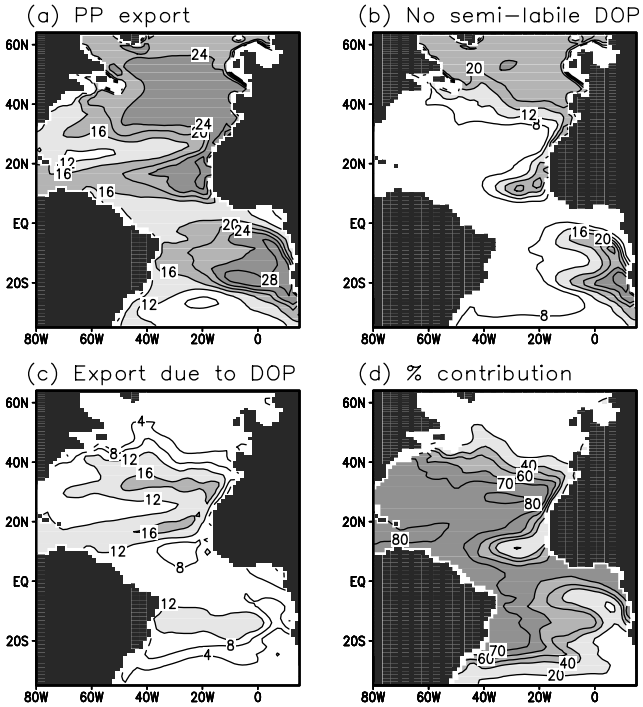

Figure 10. Model distributions for annual export of particulate organic matter (PP, mmol P m^{-2} yr^{-1}) at a depth of 100 m (a) for the default model case and (b) with no semilabile DOP included; together with (c) the PP export due to input of DOP (mmol P m^{-2} yr^{-1}) from the difference of Figures 10a and 10b, and (d) the percentage of PP export due to DOP.

are then transported into the subtropical gyre, as part of both the wind-driven Ekman circulation (Figure 11a, white arrows) and the overturning circulation. Thus the lateral transfer and cycling of DON and DOP into the euphotic zone provides alternative sources of N and P to sustain the growth of phytoplankton over the subtropical gyre.

[58] The transport of DON and DOP can contribute to closing the N and P budgets over the North Atlantic. The vertical and meridional gradients in DON and DOP are generally opposite to those of nitrate and phosphate. The overturning circulation leads to an overall southward transport of nitrate and phosphate over the North Atlantic and, conversely, a northward transport of DON and DOP (Figure 11b). Thus the overall loss of nitrate and phosphate over the North Atlantic is partly offset by the input of DON and DOP. For a steady state and plausible nitrate and phosphate distributions, the model requires external N and P sources, such as atmospheric deposition and river runoff, as well as nitrogen fixation for N alone. Our study supports the original hypothesis by *Rintoul and Wunsch* [1991] that the loss of nitrate over the subtropical North Atlantic is partly compensated by a supply of DON.

[59] A central question is how much export production over subtropical gyres is sustained through inputs of DON and DOP? If the role of DON is considered simply in terms of its contribution to PON export, then the model experiments suggest that incorporating DON transport provides an enhancement of 0.05 mol N m^{-2} yr^{-1} in PON export. This DON-induced enhancement in PON export is too small to account for the difference of typically 0.2 mol N m^{-2} yr^{-1} between traditional estimates nitrate supply and that implied from transient-tracer measurements for the Sargasso Sea [*McGillicuddy et al.*, 1998]. However, our estimate of the DON contribution to PON export is comparable to the nitrate supply of 0.05 ± 0.01 mol N m^{-2} yr^{-1} from diapycnic diffusion [*Lewis et al.*, 1986] and 0.03 mol N m^{-2} yr^{-1} from atmospheric deposition [*Knap et al.*, 1986]. It should be noted that part of the mismatch in estimates of export production could be due to errors in the measurement of particle export by sediment traps, while tracer estimates of export production include the effect of oxygen consumption from the regeneration of nitrate from both DON and PON.

[60] Concomitant with the DON transfer, there is a supply of DOP which might be more important in sustaining particle export. Our model studies suggest that the input of DOP can reach from 12 to 16 mmol P m^{-2} yr^{-1} over parts of the subtropical gyres, which sustains typically 70% of the modeled PP export. This model prediction suggesting an important role for DOP inputs over the subtropical gyres is plausible given the difficulty in supplying P to the surface

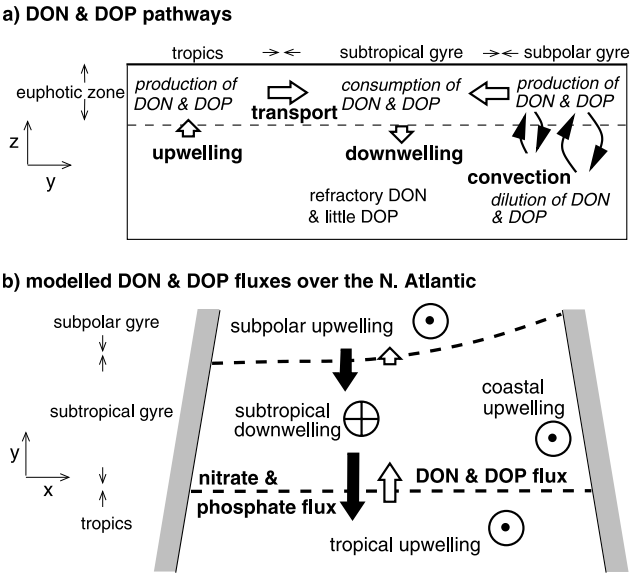

Figure 11. A schematic figure depicting (a) a meridional section showing how DON and DOP are produced in upwelling zones, then are generally concentrated within the mixed layer in the tropics and are diluted by convection at high latitudes, and finally are transported into the northern subtropical gyre where the DON and DOP are either consumed or subducted (white arrows depicting the wind-driven Ekman circulation); (b) a plan view depicting an overall southward, depth and zonally integrated flux of nitrate and phosphate from the overturning circulation (black arrows) together with a northward depth and zonally integrated flux of DON and DOP (white arrows). There is an overall loss of nitrate and phosphate over the subtropical gyre, which is partially offset by a gain in DON and DOP.

waters, since atmospheric inputs of P are weak [*Baker et al.*, 2003] and nitrogen fixation requires a P supply. In comparison, for the Sargasso Sea, tracer estimates of export production require a larger P supply of 30 ± 9 mmol P m^{-2} yr^{-1} assuming a 16:1 Redfield ratio [*Jenkins*, 1982, 1988; *Jenkins and Goldman*, 1985]. Thus our model prediction of a DOP input of 16 to 12 mmol P m^{-2} yr^{-1} might account for 40% to 50% of the observed P requirements for the Sargasso Sea.

[61] Our model results depend on a range of assumptions concerning the lifetimes and composition of the DON and DOP, such as assuming that the refractory pool of DOP is typically 5% or less. If there is a larger refractory pool of DOP, then the role of the semilabile DOP accordingly diminishes, as reflected in model sensitivity experiments for DON. Thus our model prediction that DOP plays a central role in sustaining PP export needs to tested with additional measurements of DOP across the Atlantic.

[62] In summary, the depth-integrated transport of DON and DOP is in the opposite direction to that of nitrate and phosphate, and thus partly helps to close the nutrient budgets for the subtropical North Atlantic. The inputs of DON only lead to a limited enhancement of PON export due to most of the DON being refractory. However, inputs of DOP appear to be more significant and might be sufficiently large to provide typically half of the P requirements for particle export over subtropical gyres.

[63] **Acknowledgments.** The work was supported by the UK Natural Environment Research Council through the Atlantic Meridional Transect Programme (NER/O/S/2001/01245) and a 36N Consortium grant (NER/O/S/2003/00625), and C. M. would like to acknowledge financial support from Dave Karl. We would like to thank Reiner Schlitzer for providing his inverse model estimates of export production. We are also grateful for the advice of the Associate Editor and an anonymous reviewer.

References

Abell, J., S. Emerson, and P. Renaud (2000), Distributions of TOP, TON and TOC in the North Pacific subtropical gyre: Implications for nutrient supply in the surface ocean and remineralization in the upper thermocline, *J. Mar. Res.*, *58*, 203–222.

Álvarez, M., H. L. Bryden, F. F. Perez, A. F. Rios, and G. Roson (2002), Physical and biogeochemical fluxes and net budgets in the subpolar and temperate North Atlantic, *J. Mar. Res.*, *60*, 191–226.

Baker, A. R., S. D. Kelly, K. F. Biswas, M. Witt, and T. D. Jickells (2003), Atmospheric deposition of nutrients to the Atlantic Ocean, *Geophys. Res. Lett.*, *30*(24), 2296, doi:10.1029/2003GL018518.

Benner, R. (2002), Chemical composition and reactivity, in *Biogeochemistry of Marine Dissolved Organic Matter*, edited by D. A. Hansell and C. A. Carlson, pp. 153–250, Elsevier, New York.

Bjorkman, K., A. L. Thomson-Bulldis, and D. M. Karl (2000), Phosphorus dynamics in the North Pacific subtropical gyre, *Aquat. Microb. Ecol.*, *22*, 185–198.

Bleck, R., and L. T. Smith (1990), A wind-driven isopycnic coordinate model of the North and equatorial Atlantic Ocean: 1. Model development and supporting experiments, *J. Geophys. Res.*, *95*, 3273–3285.

Bronk, D. A. (2002), Dynamics of DON, in *Biogeochemistry of Marine Dissolved Organic Matter*, edited by D. A. Hansell and C. A. Carlson, pp. 153–250, Elsevier, New York.

Bronk, D. A., and B. B. Ward (2000), Magnitude of DON release relative to gross nitrogen uptake in marine systems, *Limnol. Oceanogr.*, *45*, 1879–1883.

Bronk, D. A., P. M. Glibert, and B. B. Ward (1994), Nitrogen uptake, dissolved organic nitrogen release and new production, *Science*, *265*, 1843–1846.

Carlson, C. A. (2002), Production and removal processes, in *Biogeochemistry of Marine Dissolved Organic Matter*, edited by D. A. Hansell and C. A. Carlson, pp. 91–153, Elsevier, New York.

Cavender-Bares, K. K., D. M. Karl, and S. W. Chisholm (2001), Nutrient gradients in the western North Atlantic Ocean: Relationship to microbial community structure, and comparison to patterns in the Pacific Ocean, *Deep Sea Res., Part I*, *48*, 2373–2395.

Dietze, H., A. Oschlies, and P. Kahler (2004), Internal-wave-induced and double-diffusive nutrient fluxes to the nutrient-consuming surface layer in the oligotrophic subtropical North Atlantic, *Ocean Dyn.*, *54*, 1–7, doi:10.1007/s10236-003-0060-9.

Dittmar, T., H. P. Fitznar, and G. Kattner (2001), Origins and biogeochemical cycling of organic nitrogen in the eastern Arctic Ocean as evidence from D- and L- amino acids, *Geochim. Cosmochim. Acta*, *65*(22), 4103–4114.

Flynn, K. J., and L. S. Berry (1999), The loss of organic nitrogen during marine primary production may be significantly overestimated when using ^{15}N substrates, *Proc. R. Soc., Ser. B*, *266*, 641–647.

Gruber, N., and J. L. Sarmiento (1997), Global patterns of marine nitrogen fixation and denitrification, *Global Biogeochem. Cycles*, *11*(2), 235–266.

Hansell, D. A., and C. A. Carlson (2001), Biogeochemistry of total organic carbon and nitrogen in the Sargasso Sea: Control by convective overturn, *Deep Sea Res., Part II*, *48*, 1649–1667.

Hu, S. H., and W. O. Smith (1998), The effects of irradiance on nitrate uptake and dissolved organic nitrogen release by phytoplankton in the Ross Sea, *Cont. Shelf Res.*, *18*, 971–990.

Jenkins, W. J. (1982), Oxygen utilisation rates in North Atlantic subtropical gyre and primary production in oligotrophic systems, *Nature*, *300*, 246–248.

Jenkins, W. J. (1988), Nitrate flux into the photic zone near Bermuda, *Nature*, *331*, 521–523.

Jenkins, W. J. (1998), Studying subtropical thermocline ventilation and circulation using tritium and ^{3}He, *J. Geophys. Res.*, *103*, 15,817–15,832.

Jenkins, W. J., and J. C. Goldman (1985), Seasonal oxygen cycling and primary production in the Sargasso Sea, *J. Mar. Res.*, *43*, 465–491.

Kahler, P., and W. Koeve (2001), Marine dissolved organic matter: Can its C:N ration explain carbon overconsumption, *Deep Sea Res., Part II*, *48*, 49–62.

Karl, D. M., and K. M. Bjorkman (2002), Dynamics of DOP, in *Biogeochemistry of Marine Dissolved Organic Matter*, edited by D. A. Hansell and C. A. Carlson, pp. 91–153, Elsevier, New York.

Knap, A., T. Jickells, A. Pszenny, and J. Galloway (1986), Significance of atmospheric-derived fixed nitrogen on productivity of the Sargasso Sea, *Nature*, *320*, 158–160.

Lara, C., R. Rodriguez, and M. G. Guerrero (1993), Sodium-dependent nitrate transport and energetics of cyanobacteria, *J. Phycol.*, *29*, 389–395.

Lavín, A. M., H. L. Bryden, and G. Parrilla (2003), Mechanisms of heat, freshwater, oxygen and nutrient transports and budgets at 24.5°N in the subtropical North Atlantic, *Deep Sea Res., Part I*, *50*, 1099–1128.

Lévy, M., P. Klein, and A.-M. Tréguier (2001), Impact of sub-mesoscale physics on production and subduction of phytoplankton in an oligotrophic regime, *J. Mar. Res.*, *59*, 535–565.

Lewis, M. R., W. G. Harrison, N. S. Oakey, D. Herbert, and T. Platt (1986), Vertical nitrate fluxes in the oligotrophic ocean, *Science*, *234*, 870–873.

Loh, A. N., J. E. Bauer, and E. R. M. Druffel (2004), Variable aging and storage of dissolved organic components in the open ocean, *Nature*, *430*, 877–881.

Mahaffey, C., R. G. Williams, G. A. Wolff, and W. T. Anderson (2004), Physical supply of nitrogen to phytoplankton in the Atlantic Ocean, *Global Biogeochem. Cycles*, *18*, GB1034, doi:10.1029/2003GB002129.

McGillicuddy, D. J., A. R. Robinson, D. A. Siegel, H. W. Jannasch, R. Johnson, T. Dickeys, J. McNeil, A. F. Michaels, and A. H. Knap (1998), New evidence for the impact of mesoscale eddies on biogeochemical cycling in the Sargasso Sea, *Nature*, *394*, 263–266.

Mopper, K., X. Zhou, R. J. Kieber, D. J. Kieber, R. J. Sikirski, and R. D. Jones (1991), Photochemical degradation of dissolved organic carbon and its impact on the oceanic carbon cycle, *Nature*, *353*, 60–62.

Oschlies, A. (2002), Can eddies make ocean deserts bloom?, *Global Biogeochem. Cycles*, *16*(4), 1106, doi:10.1029/2001GB001830.

Raimbault, P., G. Slawyk, B. Boudjellal, C. Coatanoan, P. Conan, B. Coste, N. Carcia, T. Moutin, and M. Pujo-Pay (1999), Carbon and nitrogen uptake and export in the equatorial Pacific at 150°W: Evidence for an efficient regenerated production cycle, *J. Geophys. Res.*, *104*, 3341–3356.

Ridal, J. J., and R. M. Moore (1990), A re-examination of the measurement of dissolved organic phosphorus in seawater, *Mar. Chem.*, *29*, 19–31.

Rintoul, S. R., and C. Wunsch (1991), Mass, heat, oxygen and nutrient fluxes and budgets in the North Atlantic Ocean, *Deep Sea Res.*, *38*, S355–S377.

Sanders, R., and T. Jickells (2000), Total organic nutrients in Drake Passage, *Deep Sea Res., Part I*, *47*, 997–1014.

Schlitzer, R. (2000), Applying the adjoint method for biogeochemical modelling: Export of particulate organic matter in the World Ocean, in *Inverse Methods in Biogeochemical Cycles*, *Geophys. Monogr. Ser.*, vol. 114, edited by P. Kasibhata, pp. 107–124, AGU, Washington, D. C.

Sharp, J. H., et al. (2002), A preliminary methods comparison of dissolved organic nitrogen in seawater, *Mar. Chem.*, *78*, 171–184.

Thomson-Bulldis, A., and D. Karl (1998), Application of a novel method for phosphorus determinations in the oligotrophic North Pacific Ocean, *Limnol. Oceanogr.*, *43*, 1565–1577.

Usbeck, R., R. Schlitzer, G. Fisher, and G. Wefer (2003), Particle fluxes in the ocean: Comparison of sediment trap data with results from inverse modelling, *J. Mar. Syst.*, *39*, 167–183.

Varela, M. M., A. Bode, E. Fernandez, N. Gonzalez, V. Kitidis, M. Varela, and E. M. S. Woodword (2005), Nitrogen uptake and dissolved organic nitrogen release in plankton communities, characterised by phytoplankton size-structure in the central Atlantic Ocean, *Deep Sea Res., Part I*, *52*, 1637–1661.

Vidal, M., C. M. Duarte, and S. Agusti (1999), Dissolved organic nitrogen and phosphorus pools and fluxes in the central Atlantic Ocean, *Limnol. Oceanogr.*, *44*, 106–115.

Wheeler, P. A., J. M. Watkins, and R. L. Hansing (1997), Nutrients organic carbon and organic nitrogen in the upper water column of the Arctic Ocean: Implications for the sources of dissolved organic carbon, *Deep Sea Res., Part II*, *44*, 1571–1592.

Williams, R. G., and M. J. Follows (1998), The Ekman transfer of nutrients and maintenance of new production over the North Atlantic, *Deep Sea Res., Part I*, *45*, 461–489.

Williams, R. G., V. Roussenov, and M. J. Follows (2006), Nutrient streams and their induction into the mixed layer, *Global Biogeochem. Cycles*, *20*, GB1016, doi:10.1029/2005GB002586.

Wu, J., W. Sunda, E. A. Boyle, and D. M. Karl (2000), Phosphate depletion in the western North Atlantic Ocean, *Science*, *289*, 759–762.

C. Mahaffey, Department of Oceanography, University of Hawaii, 1000 Pope Road, Honolulu, HI 96822, USA.

V. Roussenov, R. G. Williams, and G. A. Wolff, Department of Earth and Ocean Sciences, University of Liverpool, Liverpool, L69 3GP, UK. (ric@liverpool.ac.uk)